TISSUE ENGINEERING: Part A
Volume 19, Numbers 9 and 10, 2013

DOI: 10.1089/ten.tea.2012.0177

Micrometer Scale Guidance of Mesenchymal Stem Cells to Form Structurally Oriented Cartilage Extracellular Matrix

Chih-Ling Chou, MS,[1] Alexander L. Rivera, BS,[2] Takao Sakai, PhD, MD,[3] Arnold I. Caplan, PhD,[4] Victor M. Goldberg, MD,[5] Jean F. Welter, PhD, MD,[4] and Harihara Baskaran, PhD[1]

Tissue engineering is a possible method for long-term repair of cartilage lesions, but current tissue-engineered cartilage constructs have inferior mechanical properties compared to native cartilage. This problem may be due to the lack of an oriented structure in the constructs at the microscale that is present in the native tissue. In this study, we utilize contact guidance to develop constructs with microscale architecture for improved chondrogenesis and function. Stable channels of varying microscale dimensions were formed in collagen-based and polydimethylsiloxane membranes via a combination of microfabrication and soft-lithography. Human mesenchymal stem cells (MSCs) were selectively seeded in these channels. The chondrogenic potential of MSCs seeded in these channels was investigated by culturing them for 3 weeks under differentiating conditions, and then evaluating the subsequent synthesized tissue for mechanical function and by type II collagen immunohistochemistry. We demonstrate selective seeding of viable MSCs within the channels. MSC aligned and produced mature collagen fibrils along the length of the channel in smaller linear channels of widths 25–100 μm compared to larger linear channels of widths 500–1000 μm. Further, substrates with microchannels that led to cell alignment also led to superior mechanical properties compared to constructs with randomly seeded cells or selectively seeded cells in larger channels. The ultimate stress and modulus of elasticity of constructs with cells seeded in smaller channels increased by as much as fourfolds. We conclude that microscale guidance is useful to produce oriented cartilage structures with improved mechanical properties. These findings can be used to fabricate large clinically useful MSC–cartilage constructs with superior mechanical properties.

Introduction

Arthritis currently affects over 49 million individuals in the United States, who suffer from severe joint pain caused by articular cartilage damage.[1] Because cartilage lacks a vascular system, it cannot recruit the necessary regenerative cells to repair these lesions.[2–4] Therefore, measures must be taken to repair cartilage lesions; however, present cartilage repair techniques appear to provide less than ideal repair tissue.[5] Tissue engineering (TE) is viewed as a promising method for long-term repair of cartilage lesions. In this approach, mesenchymal stem cells (MSCs) or chondrocytes have been combined with biodegradable scaffolds or extracellular matrix (ECM)-derived acellular scaffolds and growth factors to produce cartilage constructs *in vitro*.[6–20] TE constructs have been shown to be biochemically similar to native cartilage, however, they have inferior mechanical strength compared to native cartilage. This has been attributed to a lack of an oriented microscale structure in TE constructs, which is present in the native tissue, and prevents these constructs from reaching a clinically viable tissue.[21]

Mathematical models suggest that, within native articular cartilage, the organization of the ECM as shown in Figure 1 provides the depth-dependent mechanical strength necessary for everyday load bearing. The increase in mechanical strength from the surface of the cartilage to the deep zone is attributed to the ECM alignment.[22,23]

The goal of this study was to test the hypothesis that microscale substrate features would cause differentiating MSCs to preferentially arrange themselves and to deposit an oriented cartilage ECM on a scale similar to native articular cartilage. To reach this goal, we used contact guidance, which in previous studies, has been shown to influence cell orientation, migration, and functions.[24,25] In particular, Manwaring *et al.* showed that substrate features caused alignment of cells, which in turn could align ECM proteins.[26]

Departments of [1]Chemical Engineering and [2]Biomedical Engineering, Case Western Reserve University, Cleveland, Ohio.
[3]Department of Biomedical Engineering, Lerner Research Institute, Cleveland Clinic Foundation, Cleveland, Ohio.
[4]Department of Biology, Skeletal Research Center, Case Western Reserve University, Cleveland, Ohio.
[5]Department of Orthopaedics, Case Western Reserve University, Cleveland, Ohio.

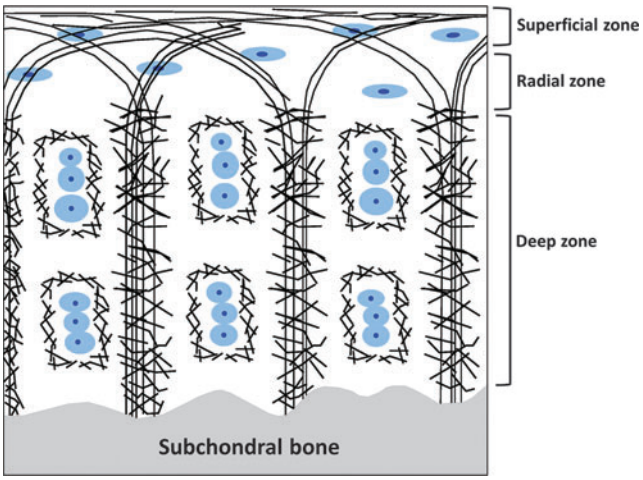

FIG. 1. Schematic of ultrastructure of articular cartilage (adapted from Hunziker*et al.*[36]): Blue circular shapes are chondrocytes and the black bands are collagen fibrils. The figure shows orthogonal arrangement of collagen fibrils in the central and near the subchondral bone regions of the cartilage and a parallel arrangement near the superficial region of the cartilage. This ultrastructure has been shown to play a role in cartilage mechanical properties.[22] Color images available online at www.liebertpub.com/tea

Despite these studies, the effects of contact guidance on stem cell differentiation and chondrogenesis are poorly understood. To our knowledge, no study has shown the effect of contact guidance on human MSC (hMSC)-based chondrogenesis; specifically, the effects of contact guidance on the synthesized type II collagen and on the mechanical properties of the resulting constructs are not known.

Using contact guidance, we formed constructs with microscale architecture for improved structure and function. Channels of varying microscale dimensions in either collagen-based or polydimethylsiloxane (PDMS) membranes were formed via a combination of microfabrication and soft-lithography. Selective seeding of viable MSCs within the channels and subsequent chondrogenic differentiation led to alignment of mature type II collagen fibrils along the length of the channel. The quality of alignment was significantly dependent on the channel dimensions; further, our results show that alignment was correlated with a significant improvement in mechanical properties.

Materials and Methods

Collagen type I from the bovine Achilles tendon, chondroitin-6-sulfate sodium salt from shark cartilage, 1-ethyl-3-(3-dimethylaminopropyl) carbodiimide hydrochloride (EDC), N-hydroxy-succinimide, fetal bovine serum (FBS), 4′,6-diamidino-2-phenylindole (DAPI), and phalloidin were purchased from Sigma Chemical Co. (St. Louis, MO). The antibiotic–antimycotic cocktail, the low-glucose Dulbecco's modified Eagle's medium (DMEM-LG), the high-glucose DMEM (DMEM-HG), ascorbate 2-phosphate (A2P), dexamethasone, sodium pyruvate, and human plasma fibronectin were obtained from Gibco, Invitrogen (Carlsbad, CA). Sylgard® silicone elastomer was purchased from Dow Corning Corporation (Midland, MI). The fibroblast growth factor-2 (FGF) and transforming growth factor β1 (TGF-β1) were purchased from Peprotech (Rocky Hill, NJ). Insulin–transferrin–selenium (ITS) + the premix tissue culture supplement were obtained from Becton Dickinson (Franklin Lakes, NJ). Carboxyfluorodiacetatesuccinimidyl ester (CFDA-SE; Vybrant®), 1,1′-dioctadecyl-3,3,3′3′-tetramethylindocarbocyanine perchlorate (DiI) cell labeling solution, calcein AM, and ethidium homodimer-1 (EthD-1) were obtained from Molecular Probes (Invitrogen, Carlsbad, CA). Pluronic F108 was purchased from BASF (Whitehouse, OH). The fluorescein isothiocyanate (FITC)-conjugated goat anti-mouse IgG secondary antibody was purchased from MP Biomedicals (Irvine, CA), while the collagen type II primary antibody was obtained from the Developmental Studies Hybridoma Bank (University of Iowa).

Collagen–glycosaminoglycan and EDC solution formation

A total of 2.20 g of type I collagen was dissolved in 800 mL of 0.5% acetic acid in diH_2O and homogenized at 13,500 RPM for 20 min in a tissue homogenizer (IKA-Works, Wilmington, NC). Next, 0.22 g of chondroitin-6-sulfate dissolved in 40 mL of 0.5% acetic acid in diH_2O was added to the homogenized collagen solution. The solution was then further homogenized at 22,000 RPM for 20 min. A crosslinking solution of EDC was made by dissolving 0.727 g of EDC and 0.063 g of N-hydroxy-succinimide in 100 mL of diH_2O and was used in the pattern formation (see below).

Design of microchannels

Templates for rectangular channels of constant length and varying widths were created using AutoCADLT (AutoDesk, San Rafael, CA) (Fig. 2A). Channels of widths 25, 50, 100, 500, and 1000 μm and length 2.5 cm were tested. The depth of the channels was maintained constant at 70 μm. To form these channels on a silicon template, standard microfabrication methods were used.[27]

Pattern formations in collagen

Collagen–glycosaminoglycan (GAG) membranes were produced using a previously published filtration method over a period of 36 h.[27] Briefly, the collagen-GAG solution is poured onto a glass filter attached to a vacuum flask. Care is taken to level the filter so that a membrane of uniform thickness can be obtained. Silicon wafers containing the patterns in Figure 2A were then used to produce channels on the surface of the collagen membranes by a technique of collagen soft-lithography that involved selective solubilization, patterning, and pattern stabilization through EDC crosslinking (Fig. 2B). To verify the widths of the channels, phase-contrast images were taken and the channel dimensions were measured through image analysis. Before cell-seeding, the membranes were incubated in 10× antibiotic–antimycotic cocktail for 1 day and 1× antibiotic–antimycotic cocktail for another day, and then washed thoroughly in phosphate-buffered saline (PBS).

Fabrication of PDMS membranes by soft-lithography

The pattern created on the silicon wafer was replicated in Sylgard silicone elastomer to make PDMS membranes.[28] The elastomer base was mixed 10:1 (w/w) with the curing agent.

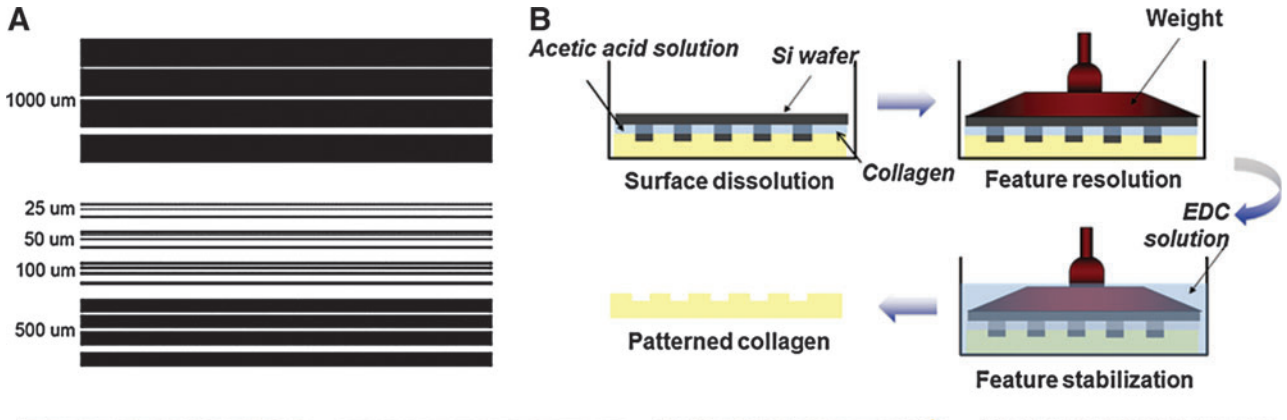

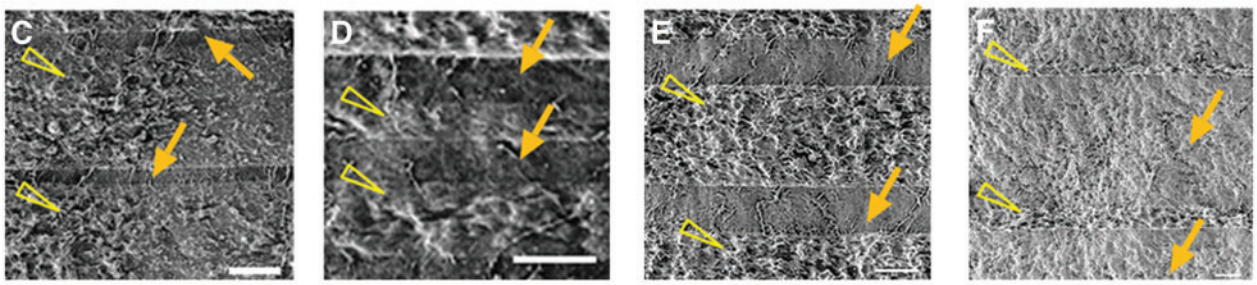

G

Design Width (μm)	Template Width Mean ± SD (μm)	Measured Channel Width Mean ± SD (μm)
25	25.7 ± 0.1	28.3 ± 0.6
50	50.4 ± 0.4	57.5 ± 0.8
100	100.2 ± 0.4	108.3 ± 0.8
500	502.0 ± 1.4	516.4 ± 1.6
1000	1007.4 ± 1.8	1016.0 ± 1.6

FIG. 2. **(A)** Microchannel design created in AutoCAD. The channels ranged from a minimum width of 25 μm to a maximum width of 1000 μm. The spacing between channels of the same width was varied from 50 to 250 μm for different designs to allow us to test the effect of channel density in future experiments. **(B)** A schematic of the process used to obtain patterns in collagen–glycosaminoglycan (GAG) membranes. **(C–F)** Scanning electron micrographs of linear channels of width 25 **(C)**, 50 **(D)**, 100 **(E)**, and 500 **(F)** μm formed in collagen-GAG membranes. Arrows point to the channels and arrowheads point to spaces between the channels. **(G)** Accuracy of channel reproduction in collagen-GAG membranes. Template width indicates the width of channels in the mask used for photolithography. Mean values of measured width ± standard deviations are shown. Ten channels from three different membranes for each channel size were used. EDC, 1-ethyl-3-(3-dimethylaminopropyl) carbodiimide hydrochloride. Color images available online at www.liebertpub.com/tea

The mixture was poured over the patterned wafer, cured at 80°C overnight, and the cured PDMS was peeled off the wafer surface.

Selective cell attachment for collagen membrane

To attach cells selectively to the channels, the plateaus on the surface of the patterned collagen (spaces between the channels) were selectively modified with Pluronic F108 by contacting the top surface of the patterned membranes with glass slides coated with the Pluronic solution (10 mg/mL) in diH_2O for 3 h (Fig. 3). MSCs in the growth medium were seeded on the membranes and were allowed to attach for 2 h, after which the membranes were washed with PBS to remove unattached cells.

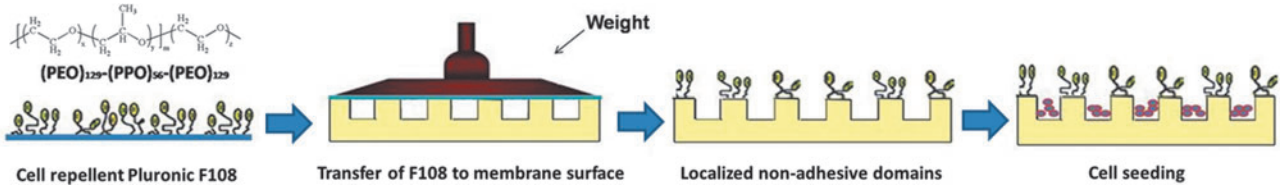

FIG. 3. A schematic of the technique used to obtain selective seeding of mesenchymal stem cells (MSCs). The steps are uniform coating of F108 on a glass coverslip, selective transfer of F108 onto nonchannel surfaces through contact with F108-coated glass, and selective seeding of MSCs in channels. Color images available online at www.liebertpub.com/tea

Selective cell attachment for PDMS membrane

PDMS membranes were exposed to oxygen plasma using a plasma etcher (SPI Plasma Prep™ II; SPI Supplies, West Chester, PA) for 30 s. The PDMS membranes were placed on a Petri dish with the channels facing down. A solution of fibronectin (10 μg/mL) in PBS was added to the Petri dish, which was placed under vacuum for 20 min to allow infiltration of the fibronectin solution into the channels of the PDMS membrane. Then, the plateaus on the surface of the patterned PDMS membrane were selectively modified with F108 as described above for the collagen membranes (Fig. 3). MSCs were seeded on the membranes and allowed to attach for 2 h. The unattached cells were then washed off with PBS. Incubation was as described above.

Cell culture

hMSCs were prepared as previously described from bone marrow aspirates obtained from healthy volunteer donors through the Stem Cell Core Facility of the Case Comprehensive Cancer Center.[29] The aspirates were harvested after informed consent under the terms of an IRB-approved protocol. We derived hMSCs from four donors; however, the cells from one donor failed to differentiate in preliminary tests, and were excluded from further experiments. Thus, cells from three individual donors were used in this study. Adult hMSCs were cultured to confluence in 1.5 g/L DMEM-LG growth medium containing 10% FBS and 10 ng/mL FGF-2. The MSCs were then trypsinized and resuspended at $\sim 50 \times 10^6$ cells/mL. The cell suspension was applied to the channels using a micropipette. After 2 h at 37°C and 5% CO_2 to allow for cell attachment, the seeded membranes were submerged in the chondrogenic differentiation medium: 4.5 g/L DMEM-HG supplemented with 10% ITS+Premix Tissue Culture Supplement, 10^{-7} M dexamethasone, 1 μM A2P, 1% sodium pyruvate, and 10 ng/mL TGF-β1.The constructs were cultured in a standard incubator at 37°C and 5% CO_2 in humidified air. The medium was changed every 2–3 days.

MSC visualization, viability, and adhesion assessment

To evaluate cell viability within the channels 1 day after seeding, Live/Dead™ staining with calcein-AM and EthD-1, along with fluorescent microscopy, was used following the manufacturer's instructions. Fluorescent images were taken and viability was quantified by evaluating the percentage of the total number of cells stained positive for calcein-AM. To improve visualization of the cells on the substrates and to visualize the cytoskeleton, various samples were stained by using CFDA-SE, DiI, and phalloidin (actin staining) following the manufacturer's instructions.

Histology and immunohistochemistry

After culturing for 21 days, some samples were fixed in 4% neutral-buffered formaldehyde. Whole-mounts were surface-stained for type II collagen by immunohistochemistry. Antigen unmasking was performed with 1 mg/mL pronase in PBS for 15 min at room temperature. After washing the samples with PBS twice for 30 min, they were then blocked with 10% normal goat serum (NGS) in PBS for 30 min. The primary antibody diluted 1:50 in 1% NGS in PBS, was applied to the samples for 1 h to stain for collagen type II. The samples were then washed with PBS (2×30 min). The FITC-conjugated goat anti-mouse IgG secondary antibody, diluted 1:500 in 1% NGS in PBS, was then applied to the samples for 45 min. All samples were counterstained with DAPI to visualize the cell nuclei. Some samples were counterstained with DiI for membrane staining and some samples were stained with phalloidin for actin following the respective manufacturer's instructions. The samples were again washed with PBS for 1 h, counterstained, and wet-mounted using 5% N-propyl gallate in glycerol. The samples were imaged either using a SPOT RT digital camera attached to a Leica fluorescence microscope (Wetzlar, Germany) or by confocal microscopy (Zeiss LSM 510, Zeiss Axiovert 200M; Carl Zeiss, Thornwood, NY).

Cell alignment analysis

To obtain a quantitative measure of alignment, the acute angle of the nuclei was calculated relative to the direction of the channel length. At least three images from three separate experiments were used and frequency histograms of the angles were plotted. An alignment angle of 0° indicates perfect alignment with the long dimension of the channels and an angle of 90° indicates perfect alignment with the short dimension of the channels.

Biochemical measurements

We determined the GAG and DNA content of the tissue formed during chondrogenesis using previously published methods.[29] Briefly, the cartilaginous tissue formed was digested using papain (Sigma Chemical Co.). The DNA content was measured from the fluorescence of papain-digested samples after combining with Hoechst 33258 (Sigma Chemical Co., excitation wavelength 340 nm and emission wavelength 465 nm). Calf thymus DNA standards were used (Amersham Biosciences, Piscataway, NJ). The GAG content was measured colorimetrically after combining the samples with Safranin-O and reading the absorbance at 530 nm. Shark cartilage chondroitin sulfate C samples (Seikagaku America, East Falmouth, MA) were used as standards.

Mechanical tests

To determine whether alignment led to improved function, the collagen membrane samples were subjected to tensile testing. For each mechanical testing sample, only a single channel size was used and the spacing between channels was equivalent to the channel width (projected channel area was 50% of the total surface area for all channel sizes). Therefore, the seeding areas of the channels and the seeding densities were identical for each sample. In addition, the ratio of the channel cross-sectional area containing tissue to the total sample cross-sectional area was constant for every condition and was 0.1 based on a membrane depth of 400 μm. Collagen membranes with hMSCs cultured for 21 days under differentiating conditions were cut to half using a razor blade to rectangular dimensions of $\sim$9 mm length×5 mm width×0.45 mm thickness. The collagen membranes were not degradable in the cell culture medium; therefore, the base membranes of all samples subjected to mechanical testing were consistent. The edge of the sample was gripped with film tension clamps and subjected to tensile strain in a

dynamic mechanical analysis apparatus (QA800; TA Instruments, New Castle, DE) along the direction of channel length until failure. Strain was ramped from 20%/min to 200%/min. Stress (σ) vs. strain (ε) data were obtained and fitted to the equation $\sigma = a\ (e^{b\varepsilon} - 1)$ to yield the modulus of elasticity (ab).[11,30] Ultimate stress values were calculated at the failure point. At least seven samples were used per condition tested.

Statistical methods

Statistical analysis was carried out using the Origin 8.5.1 (Origin Lab, Northampton, MA) software package. Pairwise comparisons were made using the Tukey's test with a p-value of less than 0.05 considered statistically significant. Sample sizes are indicated in the respective figure legends.

Results

Collagen membrane patterning

Figure 2G shows the accuracy of the collagen soft-lithography method in reproducing the channel designs. The measured widths of the features in the template and the collagen membrane are shown along with the expected design values. The relative error between the membrane channel widths and the template widths ranged from 1 to 15%, indicating that our EDC-based collagen soft-lithography method for forming patterned collagen membranes is robust and accurate for forming channels as small as 25 μm.

Selective cell attachment

Cell viability on collagen membranes evaluated by Live/Dead® staining followed by image analysis was >95%. Qualitatively, the cells adhered well located and spread on the collagen surface (Data not shown). Without Pluronic treatment, cells adhered both inside and outside the channels in both collagen and PDMS substrates (Fig. 4 and 5). Using the Pluronic treatment on collagen and PDMS led to significantly more selective adhesion of cells within the channels (Figs. 4A–C and 5A–E). These results indicate the importance of the Pluronic modification to achieve selective cell attachment within the channels. When comparing selective attachment of collagen *vs.* PDMS membranes, the latter yielded better in-channel attachment (Figs. 4A–C vs. 5A–E).

Microscale guidance on cell alignment

More MSC alignment along the length of the channel occurred in the smaller channels (Fig. 6A–C) compared to the larger channels (Fig. 6D, E). DAPI staining showed that the nuclei of the MSCs elongated into an oval shape in the smaller channels. Actin fibers also aligned with the long dimension of the smaller channels [Fig. 6F, H(i)]. Within the larger channels, MSCs showed random spatial orientation and less nuclear elongation [Fig. 6G, H(ii)]. Table 1 shows the angle of nuclear alignment within the channels (mean ± SEM). Figure 7 shows the distribution of angles for all conditions.

The angle measurements suggest that the smaller channels (25–100 μm) aided in cell alignment, whereas the larger (500–1000 μm) channels did not. Both collagen and PDMS substrates followed this trend. There was significant difference in alignment as measured by the angle, between 25–100-μm-wide substrates when compared with 500–1000-μm-wide substrates (the Tukey's test, $p < 0.05$). In addition, there was no significant difference in alignment between 500- and 1000-μm-wide substrates. In the larger channels, small regions in which the MSCs aligned to each other were noted (Fig. 6G), but the alignment was not in reference to the channel dimensions.

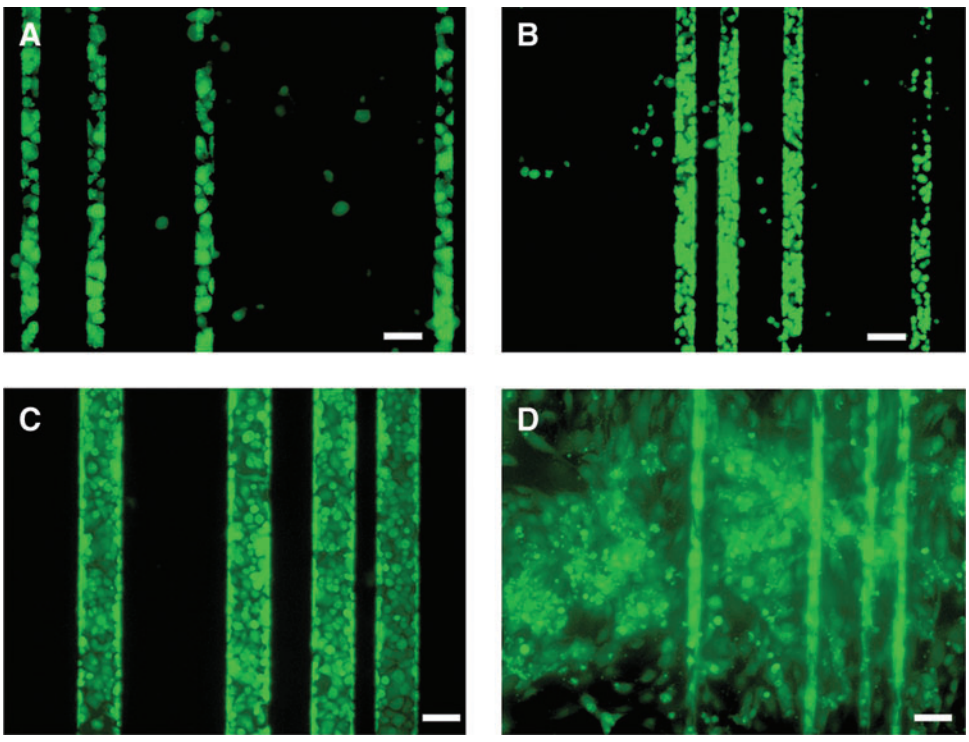

FIG. 4. Effect of F108 on selective seeding of human MSCs in polydimethylsiloxane (PDMS) microchannels. MSCs prestained with Vybrant® were seeded on to F108-treated PDMS linear channels overnight. Fluorescent images of cells in linear channels of widths 25 μm **(A)**, 50 μm **(B)**, and 100 μm **(C)** show selective seeding compared to untreated channel surfaces **(D)**. Scale bars: 50 μm **(A, D)**, 100 μm **(B, C)**. Color images available online at www.liebertpub.com/tea

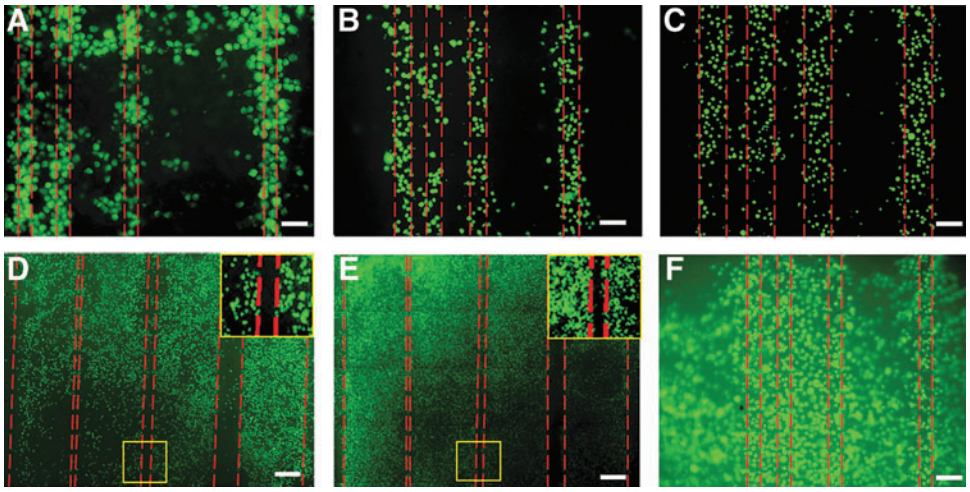

FIG. 5. Effect of F108 selective seeding of human MSCs in collagen microchannels. MSCs prestained with Vybrant were seeded onto F108-treated collagen linear channels overnight. Fluorescent images of cells in linear channels of widths 25 μm **(A)**, 50 μm **(B)**, 100 μm **(C)**, 500 μm **(D)**, and 1000 μm **(E)** show selective seeding compared to untreated channel surfaces **(F)**. Insets in **(D)** and **(E)** show magnified portions of gaps (50 μm) between the channels devoid of cells. Scale bars: 50 μm **(A, B, F)**, 100 μm **(C)**, 200 μm **(D)**, 400 μm **(E)**. Color images available online at www.liebertpub.com/tea

ECM production

Our results (Fig. 6A–E, I, J) show that mature extracellular type II collagen was deposited and that production closely followed the aligned cell in the channels. Longer type II collagen fibers are seen farther from the cell, indicating that filament assembly occurs. In the 25-, 50-, and 100-μm channels (Fig. 6A–C, I), the type II collagen aligned along the direction of the channel, while in 500- and 1000-μm channels, the type II collagen was randomly aligned (Fig. 6D, E, J). Biochemical assay results show that the GAG/DNA content in microchannels was significantly greater than that when cells were seeded on membranes with no channels (Table 2). There was, however, no difference in the GAG/DNA content between membranes of different channel widths.

Mechanical properties

Figure 8 shows the modulus of elasticity (Fig. 8A) and ultimate stress (Fig. 8B) of various collagen samples when they were subjected to tension along the direction of the channel length. Collagen membranes containing hMSCs in

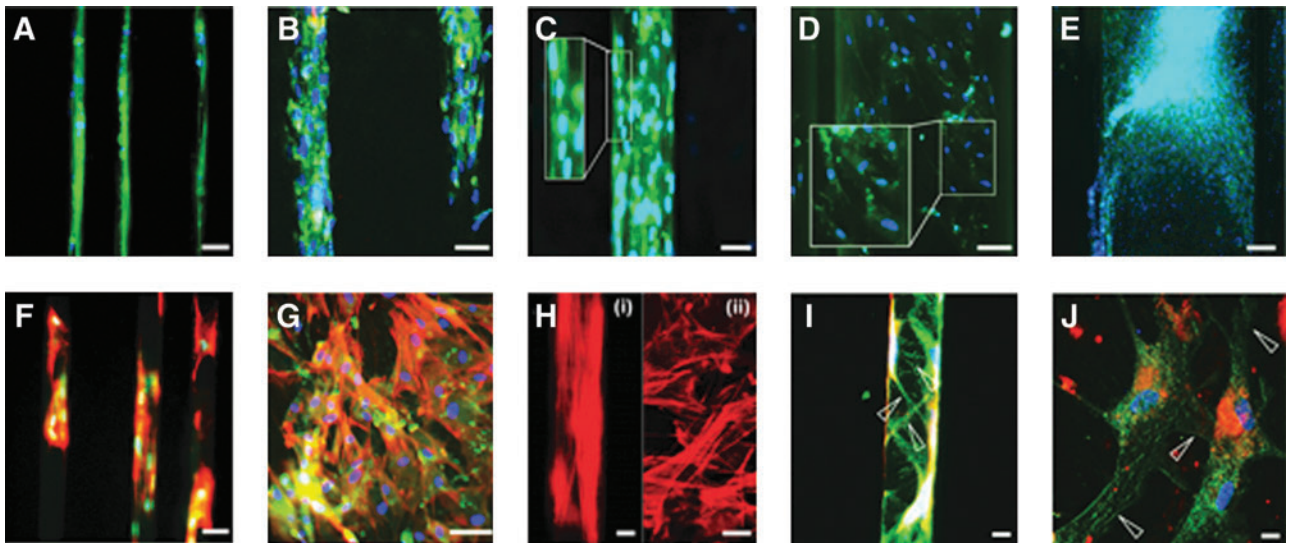

FIG. 6. Chondrogenesis under microscale guidance. Fluorescent images of linear channels of widths 25 μm **(A)**, 50 μm **(B)**, 100 μm **(C)**, 500 μm **(D)**, and 1000 μm **(E)** show alignment in smaller 25–100 μm channels. Cell nuclei alignment (blue) is correlated with actin (red) alignment in smaller channels. Insets in **(C)** and **(D)** show magnified portions of channels with cells. **[F, H(i)]** show actin alignment in linear channels of width 25 μm, which was contrasted with random alignment of actin filaments in linear channels of width 500 μm **[G, H(ii)]**. Confocal fluorescent images (green is type II collagen, blue is DAPI, and red is DiI) of 25 **(I)** and 1000 μm **(J)** channels show mature aligned extracellular matrix (arrowheads) in the smaller channel. Scale bars: 10 μm **[H(i), H(ii), I, J]**, 25 μm **(F, G)**, 50 μm **(A–C)**, 100 μm **(D)**, 200 μm **(E).** Color images available online at www.liebertpub.com/tea

Table 1. Cell Alignment Angle During Contact Guidance

Channel width (μm)	*25*	*50*	*100*	*500*	*1000*
PDMS	3.7 ± 1.4[a]	12.7 ± 2.4[a]	4.6 ± 1.0[a]	29.2 ± 2.8	32.2 ± 4.2
Collagen	4.5 ± 0.8[a]	4.1 ± 0.6[a]	8.6 ± 1.0[a]	41.8 ± 2.5	42.3 ± 3.0

Angle between the linear channel dimension and cell major axis through the cell nucleus was quantified and shown as mean ± SEM for channels of various widths. For smaller channels (25, 50, 100 μm), six channels chosen from three different experiments were used for quantitation. For larger channels (500, 1000 μm), three channels from three different experiments were used. Cells from three donors were used in the experiments. Corresponding immunofluorescence data are shown in Figure 6A–E.

[a]Statistically significant ($p < 0.05$) compared to 500- and 1000-μm-wide channels.

PDMS, polydimethylsiloxane.

the smaller channels (Fig. 8: 25, 50, 100, 250) cultured for 21 days under differentiating conditions had significantly superior mechanical properties compared to corresponding membranes with larger channels (Fig. 8: 500, 1000). Importantly, membranes with randomly seeded cells (Fig. 8A: Ran), while better than membranes with no cells (Fig. 8A: EDC), had inferior modulus of elasticity compared to membranes containing cells in channels of 25, 50, 100, and 250 μm widths (Fig. 8A: 25, 50, 100, 250). The ultimate stress data for membranes containing cells in channels of 25, 50, and 100 μm widths (Fig. 8B: 25, 50, 100) are significantly greater compared with membranes with no channels, and membranes with 250, 500, and 1000 μm-wide channels (Fig. 8B: Ran, 250, 500, 1000). There was no difference in the mechanical properties between cell-free membranes with 25- and 100-μm channels (Fig. 8: C25 and C100) and cell-free membranes with no channels (Fig. 8: EDC).

Discussion

Collagen membrane patterning

The native microstructure of articular cartilage contributes to its strength and durability.[22,23] Current TE protocols tend to produce a tissue that, while biochemically similar to cartilage, is amorphous and lacks structural similarity to the authentic tissue. The goal of this study was to investigate whether micrometer-sized guidance features in the scaffold material can be used to impose orientation upon differentiating MSCs and the ECM they produce. To control the ECM microstructure of differentiating MSCs, microscale channels in PDMS and collagen substrates were produced. While PDMS soft-lithography is well-established, in this study, a process of collagen soft-lithography combined with EDC crosslinking to create channels within collagen membranes is presented. The method employs computer-generated designs; any two-dimensional (2D) microdesigns can be replicated in collagen substrates. This method allowed for the production of stable physical features. Further, by employing EDC crosslinking, the cytotoxic effects of the typical glutaraldehyde crosslinkers, and glutaraldehyde-induced autofluorescence, a major problem in applying fluorescence-based cell labeling and tracking, are avoided.[31]

Selective cell attachment

To study the effects of the guidance channels on cellular orientation and function, the MSCs must be localized within the channels. Our protocol allows us to localize cells within the physical features of a substrate by using Pluronic F108 to resist cell attachment. Pluronic F108 is nontoxic to cells, and the new technique allows for highly improved selectivity. Contacting the Pluronic F108-coated glass slides onto the patterned collagen membranes coats only the plateau regions with Pluronic F108.For use on collagen substrates, our method is more efficient than the methods of Wang and Ho, which were developed for plastic and glass substrates.[32] By localizing the cells within the channels, constructs can be created that use the channels to guide the cell structure and function, while avoiding cell attachment outside of the channels. In this study, excellent channel-selective cell attachment was achieved within PDMS membranes and collagen membranes. However, the collagen channels showed less cellular attachment selectivity when compared to the

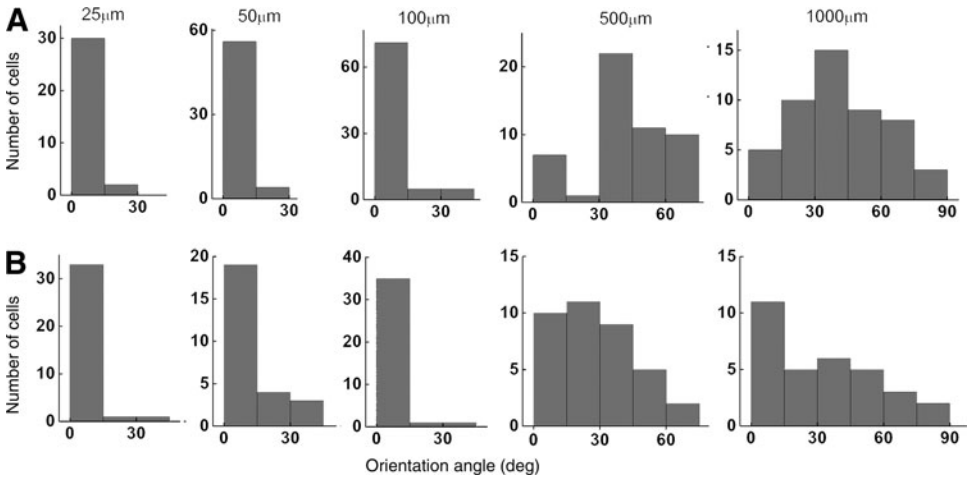

FIG. 7. Cell orientation under microscale guidance. Distribution of angles of orientation of human MSCs formed against the longer dimension of the PDMS **(A)** and collagen **(B)** channels of widths 25–1000 μm. For smaller channels (25, 50, 100 μm), six channels from three different samples were used. For larger channels (500, 1000 μm), three channels from three different samples were used. Cells from three donors were used.

Table 2. GAG and DNA Content of Cartilage Tissue Grown in the Channels

Channel width (μm)	*GAG(μg)*	*DNA(μg)*	*GAG/DNA*
25	4.3 ± 0.5	2.1 ± 0.03	2.0 ± 0.27[a]
50	4.4 ± 0.4	2.1 ± 0.01	2.1 ± 0.17[a]
100	4.0 ± 0.1	2.0 ± 0.01	2.0 ± 0.07[a]
250	3.4 ± 0.2	2.0 ± 0.05	1.7 ± 0.09[a]
500	3.3 ± 0.1	2.1 ± 0.03	1.6 ± 0.03[a]
1000	3.3 ± 0.1	2.1 ± 0.02	1.6 ± 0.05[a]
No channel	3.0 ± 0.3	2.4 ± 0.04	1.2 ± 0.09

Data from three samples from three different experiments are presented as mean ± SEM. Cells from three donors were used in the experiments.

[a]Statistical significant difference at $p < 0.05$.

GAG, glycosaminoglycan.

PDMS channels. We speculate that this difference occurred due to the superior ability of the collagen to facilitate cellular attachment, which makes the selective seeding process through F108 somewhat less effective.

MSC orientation

We hypothesized that channels in the collagen and PDMS membranes would control cellular orientation and ECM production *via* contact guidance. Our results indicate that this is the case in the smaller channels (25, 50, and 100 μm), as these lead to overall MSC alignment along the channel length. The larger channels, on the other hand, had small regions in which the MSCs are aligned to each other (Fig. 6) but not in reference to the channel dimensions. Overall, the distribution of the MSCs was random in these larger channels. The smaller scale features (25–50 μm) were close to the dimensions of the cells, and can thus guide adhesion and spreading at the single-cell level. Since EDC-crosslinked collagen has been shown to degrade substantially slower than uncrosslinked collagen substrates, the guidance effect can not only persist throughout the 3-week chondrogenesis period *in vitro*, but potentially also *in vivo*.[33] One manifestation of the cellular alignment was the orientation of actin fibers (Fig. 6). The actin–myosin network is implicated in cell-spreading and migration. Alignment of actin fibers in the small channels thus indicates guidance at the cytoskeletal level. A further indication of alignment was the elongation and orientation of the nuclei parallel to the channel axis (Fig. 6). If the cell alignment is principally due to contact guidance through confinement by the substrate surfaces that are in contact with the cell, as suggested by our findings in the 25–100-μm-wide channels, it is possible that the alignment can be propagated from cell to cell for some distance.

ECM production and orientation

The effect of guidance channels on the ECM assembly was examined using type II collagen immunohistochemistry. Our results indicate that the type II collagen observed was indeed extracellular in nature. On collagen membranes, the type II collagen immunoreactivity was clearly outside of the cell membrane, and even 100-μm channels (which are up to approximately five cell bodies wide) showed alignment (angles of alignment 4.6° for PDMS and 8.6° for collagen substrates, Table 1) with the principal axis of the channel. The fiber structure of the type II collagen present suggests that it was also extracellular in nature.

Mechanical function

Native cartilage has been shown to have a collagen architecture that imparts mechanical strength under compression and shear. In the 2D architecture of collagen membranes, we were able to demonstrate alignment, but the geometry of the samples was unsuitable for compressive testing. The mechanical properties of the samples under tension, however, indicate a strong dependence on

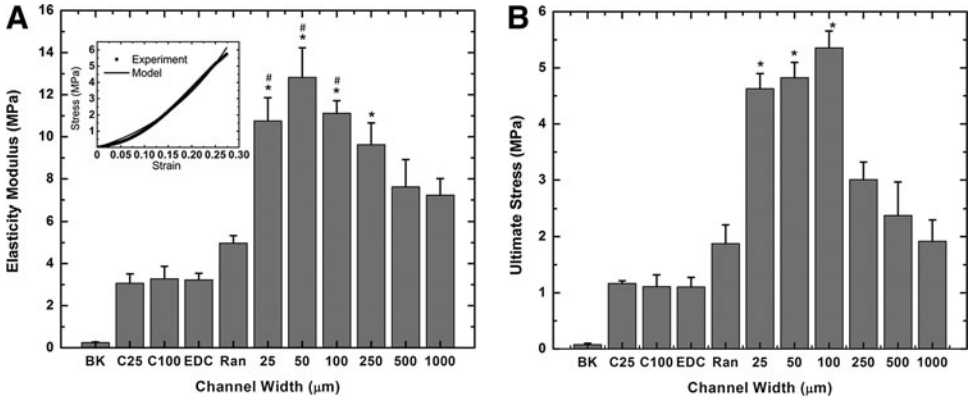

FIG. 8. Effect of microscale guidance on mechanical properties. Collagen membranes were subject to tensile testing until failure. Mean values of elasticity modulus **(A)**, a typical force–displacement curve **(A:** upper left corner**)**, and ultimate stress **(B)** are shown. BK and EDC represent, respectively, uncrosslinked and EDC crosslinked collagen membranes without microchannels or MSCs. C25 and C100 represent collagen membranes consisting of 25- and 100-μm linear channels only, without MSCs. All other channels were seeded with MSCs. Ran: EDC crosslinked collagen membranes without channels; 25, 50, 100, 250, 500, and 1000 represent widths (μm) of linear channels in the EDC crosslinked collagen membranes. $n = 4$ for 1000, $n = 5$ for Ran, C25 and C100 and $n = 6$ for all other conditions. **(A)** *Statistically significant difference ($p < 0.05$) compared to data with no channels (RAN). #Statistically significant difference ($p < 0.05$) compared to data with 1000-μm channels (1000). **(B)** *Statistically significant difference ($p < 0.05$) compared to data with no channels (RAN), 250-μm (250), 500-μm (500), and 1000-μm (1000)-wide channels. Cells from two donors used in the above experiments.

alignment. Samples containing guidance features at the cellular scale led to superior mechanical function in the presence of cells. It should be noted (Fig. 8) that the channels themselves did not, at any channel width, improve the mechanical properties of the membranes. In addition, the GAG/DNA values for constructs of different channel widths were similar indicating that differences in the GAG content between conditions were not responsible for changes in mechanical properties of tissue cultured in different channels. This suggests that the cell-derived ECM under guidance accounts for the superior function. The average tensile modulus for native articular cartilage is $\sim$0.7–12.5MPa.[34,35] The elasticity modulus for the construct containing smaller channels (25 to 250 μm) was $\sim$9.6 to 12.8 MPa which is comparable to the highest value found in the literature for native articular cartilage (12.5 MPa). On the other hand, the elasticity modulus of the construct with randomly seeded MSCs was around 5 MPa, which is comparable to the inner annulus fibrosus (3 MPa). Thus, using these guidance channels, we can produce cartilage constructs with a range of tensile properties similar to native articular cartilage.

While the above study demonstrates that microscale guidance has an effect on hMSC differentiation and on the mechanical function of the resulting tissue, there are certain limitations. First, even though we have imposed some organization on the newly synthesized ECM, we do not yet replicate the fine structure or the mechanical function of native articular cartilage. Further, more work is needed to extend the current 2D findings to a 3D construct for preclinical experiments. To create a 3D construct for *in vivo* applications, one can simply roll the current 2D constructs into 3D cylinders with appropriate microfeatures. In addition, one can also stack individual 2D constructs with MSCs in between the layers. These 3D constructs can then be implanted into the site of articular cartilage injury *in vivo.*

Conclusions

In this work, the effect of microscale guidance on cell alignment and ECM function in a hMSC-based chondrogenesis model was investigated. Microchannels formed in collagen and PDMS were utilized to show that MSCs cultured within the linear channels of smaller widths show alignment. Further, the alignment of cells and ECM leads to significant improvement in mechanical function. These results can be used to develop cartilage constructs with an aligned ECM and superior mechanical properties.

Acknowledgments

We thank Dr. Don Lennon, and Lori Duesler of the Skeletal Resource Center, Department of Biology, Case Western Reserve University, Cleveland, OH for help with the MSC isolation and culture, and immunohistochemistry, respectively. The above work was funded by a grant from the National Institutes of Health (AR053622). Mr. Rivera is supported in part by the National Science Foundation Graduate Research Fellowship under Grant No. 0951783.

Disclosure Statement

The authors declare that no competing financial interests exist.

References

1. CDC. Prevalence of doctor-diagnosed arthritis and arthritis-attributable activity limitation–United States, 2007–2009. Morbid Mortal Week Rep **59,** 1261, 2010.
2. Friedenstein, A.J. Marrow stromal fibroblasts. Calcif Tissue Int **56,** S17, 1995.
3. Caplan, A.I., Elyaderani, M., Mochizuki, Y., Wakitani, S., and Goldberg, V.M. Principles of cartilage repair and regeneration. Clin Orthop Relat Res **342,** 254, 1997.
4. Caplan, A.I., and Goldberg, V.M. Orthopaedic tissue engineering—editorial comment. Clin Orthop Relat Res **367,** S2, 1999.
5. Gilbert, J.E. Current treatment options for the restoration of articular cartilage. Am J Knee Surg **11,** 42, 1998.
6. Chung, C., and Burdick, J.A. Influence of three-dimensional hyaluronic acid microenvironments on mesenchymal stem cell chondrogenesis. Tissue Eng Part A **15,** 243, 2009.
7. Dickhut, A., Gottwald, E., Steck, E., Heisel, C., and Richter, W. Chondrogenesis of mesenchymal stem cells in gel-like biomaterials *in vitro* and *in vivo*. Front Biosci **13,** 4517, 2008.
8. Djouad, F., Mrugala, D., Noel, D., and Jorgensen, C. Engineered mesenchymal stem cells for cartilage repair. Regen Med **1,** 529, 2006.
9. Jakobsen, R.B., Shahdadfar, A., Reinholt, F.P., and Brinchmann, J.E. Chondrogenesis in a hyaluronic acid scaffold: comparison between chondrocytes and MSC from bone marrow and adipose tissue. Knee Surg Sports Traumatol Arthrosc **18,** 1407, 2010.
10. Janjanin, S., Li, W.J., Morgan, M.T., Shanti, R.M., and Tuan, R.S. Mold-shaped, nanofiber scaffold-based cartilage engineering using human mesenchymal stem cells and bioreactor. J Surg Res **149,** 47, 2008.
11. Liang, W.H., Kienitz, B.L., Penick, K.J., Welter, J.F., Zawodzinski, T.A., and Baskaran, H. Concentrated collagen-chondroitin sulfate scaffolds for tissue engineering applications. J Biomed Mater Res A **94,** 1050, 2010.
12. Salinas, C.N., and Anseth, K.S. Mesenchymal stem cells for craniofacial tissue regeneration: designing hydrogel delivery vehicles. J Dent Res **88,** 681, 2009.
13. Spadaccio, C., Rainer, A., Trombetta, M., Vadala, G., Chello, M., Covino, E., Denaro, V., Toyoda, Y., and Genovese, J.A. Poly-l-lactic acid/hydroxyapatite electrospun nanocomposites induce chondrogenic differentiation of human msc. Ann Biomed Eng **37,** 1376, 2009.
14. Wang, Y., Kim, U.J., Blasioli, D.J., Kim, H.J., and Kaplan, D.L. *In vitro* cartilage tissue engineering with 3D porous aqueous-derived silk scaffolds and mesenchymal stem cells. Biomaterials **26,** 7082, 2005.
15. Wang, Y.Z., Blasioli, D.J., Kim, H.J., Kim, H.S., and Kaplan, D.L. Cartilage tissue engineering with silk scaffolds and human articular chondrocytes. Biomaterials **27,** 4434, 2006.
16. Francioli, S.E., Candrian, C., Martin, K., Heberer, M., Martin, I., and Barbero, A. Effect of three-dimensional expansion and cell seeding density on the cartilage-forming capacity of human articular chondrocytes in type II collagen sponges. J Biomed Mater Res Part A **95A,** 924, 2010.
17. Gong, Y.Y., Xue, J.X., Zhang, W.J., Zhou, G.D., Liu, W., and Cao, Y. A sandwich model for engineering cartilage with acellular cartilage sheets and chondrocytes. Biomaterials **32,** 2265, 2011.
18. Xue, J.X., Gong, Y.Y., Zhou, G.D., Liu, W., Cao, Y., and Zhang, W.J. Chondrogenic differentiation of bone marrow-derived mesenchymal stem cells induced by acellular cartilage sheets. Biomaterials **33,** 5832, 2012.

19. Yang, Q., Peng, J., Guo, Q., Huang, J., Zhang, L., Yao, J., Yang, F., Wang, S., Xu, W., Wang, A., and Lu, S. A cartilage ECM-derived 3-D porous acellular matrix scaffold for *in vivo* cartilage tissue engineering with pkh26-labeled chondrogenic bone marrow-derived mesenchymal stem cells. Biomaterials **29,** 2378, 2008.
20. Zwingmann, J., Mehlhorn, A.T., Suedkamp, N., Stark, B., Dauner, M., and Schmal, H. Chondrogenic differentiation of human articular chondrocytes differs in biodegradable pga/pla scaffolds. Tissue Eng **13,** 2335, 2007.
21. Bhosale, A.M., and Richardson, J.B. Articular cartilage: structure, injuries and review of management. Br Med Bull **87,** 77, 2008.
22. Shirazi, R., Shirazi-Adl, A., and Hurtig, M. Role of cartilage collagen fibrils networks in knee joint biomechanics under compression. J Biomech **41,** 3340, 2008.
23. Wilson, W., Huyghe, J.M., and van Donkelaar, C.C. Depth-dependent compressive equilibrium properties of articular cartilage explained by its composition. Biomech Model Mechanobiol **6,** 43, 2007.
24. Dickinson, R.B., Guido, S., and Tranquillo, R.T. Biased cell-migration of fibroblasts exhibiting contact guidance in oriented collagen gels. Ann Biomed Eng **22,** 342, 1994.
25. Tessier-Lavigne, M., and Goodman, C.S. The molecular biology of axon guidance. Science **274,** 1123, 1996.
26. Manwaring, M.E., Walsh, J.F., and Tresco, P.A. Contact guidance induced organization of extracellular matrix. Biomaterials **25,** 3631, 2004.
27. Janakiraman, V., Kienitz, B.L., and Baskaran, H. Lithography technique for topographical micropatterning of collagen-glycosaminoglycan membranes for tissue engineering applications. J Med Devices **1,** 233, 2007.
28. Whitesides, G.M., Ostuni, E., Takayama, S., Jiang, X., and Ingber, D.E. Soft lithography in biology and biochemistry. Annu Rev Biomed Eng **3,** 335, 2001.
29. Welter, J.F., Solchaga, L.A., and Penick, K.J. Simplification of aggregate culture of human mesenchymal stem cells as a chondrogenic screening assay. Biotechniques **42,** 732, 2007.
30. Woo, S.L.Y., Akeson, W.H., and Jemmott, G.F. Measurements of nonhomogeneous, directional mechanical properties of articular cartilage in tension. J Biomech **9,** 785, 1976.
31. Gendler, E., Gendler, S., and Nimni, M.E. Toxic reactions evoked by glutaraldehyde-fixed pericardium and cardiac valve tissue bioprosthesis. J Biomed Mater Res **18,** 727, 1984.
32. Wang, Y.C., and Ho, C.C. Micropatterning of proteins and mammalian cells on biomaterials. FASEB J **18,** 525, 2004.
33. Yahyouche, A., Zhidao, X., Czernuszka, J.T., and Clover, A.J. Macrophage-mediated degradation of crosslinked collagen scaffolds. Acta Biomater **7,** 278, 2011.
34. Almarza, A.J., and Athanasiou, K.A. Design characteristics for the tissue engineering of cartilaginous tissues. Ann Biomed Eng **32,** 2, 2004.
35. Huang, C.Y., Stankiewicz, A., Ateshian, G.A., and Mow, V.C. Anisotropy, inhomogeneity, and tension-compression nonlinearity of human glenohumeral cartilage in finite deformation. J Biomech **38,** 799, 2005.
36. Hunziker, E.B., Michel, M., and Studer, D. Ultrastructure of adult human articular cartilage matrix after cryotechnical processing. Microsc Res Tech **37,** 271, 1997.

Address correspondence to:
Harihara Baskaran, PhD
Department of Chemical Engineering
Case Western Reserve University
111C, A.W. Smith Building
2102 Adelbert Road
Cleveland, OH 44106-7217

E-mail: hari@case.edu

Received: March 19, 2012
Accepted: November 14, 2012
Online Publication Date: December 26, 2012